ACS Macro Letters

Letter

pubs.acs.org/macroletters

Microstructure Analysis and Model Discrimination of Enzyme-Catalyzed Copolyesters

Matthew T. Hunley,[†] Nese Sari,[‡] and Kathryn L. Beers*[,†]

[†]Materials Science and Engineering Division, National Institute of Standards and Technology, Gaithersburg, Maryland 20899, United States

[‡]Institute of Bioscience and Biotechnology Research, University of Maryland, Rockville, Maryland 20850, United States

Supporting Information

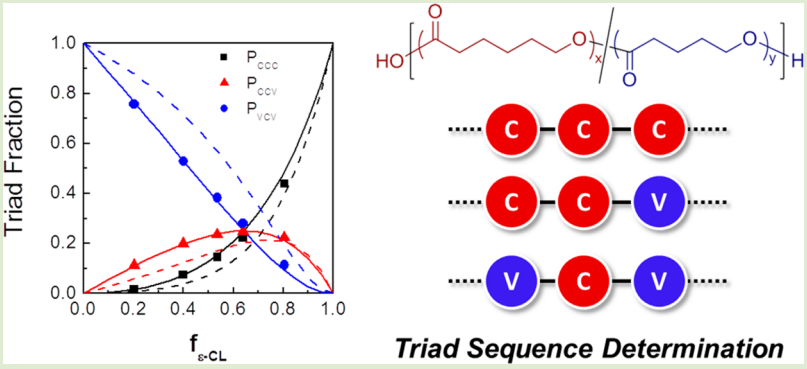

ABSTRACT: The comonomer sequence distributions were analyzed for a series of poly(ε-caprolactone-*co*-δ-valerolactone) (PCV) copolymers using ^{13}C nuclear magnetic resonance (NMR) spectroscopy. The four dyad sequences each showed well-resolved peaks in the NMR spectra that allowed easy quantification of the dyad and triad fractions. Although compositional analysis could not discriminate between terminal and penultimate model copolymerization kinetics, the monomer sequence distributions clearly indicated that the lipase-catalyzed copolymerization proceeds via terminal model kinetics. This NMR analytical tool enables rapid characterization of lipase-catalyzed copolymers.

Recent advances in the control of lipase-mediated polymerizations have demonstrated that these biocatalysts afford polyesters and polycarbonates rapidly under mild conditions.[1] Transesterification polycondensation and ring-opening polymerizations (ROP) both occur through the formation of enzyme-activated monomers, and the kinetics of these polymerizations have been thoroughly studied.[2−4] Compared to conventional metal catalysts, the lipase catalysts can improve the environmental impact of ROP by eliminating the need for heavy metals and reducing the energy consumption for high temperature reactions. Certain lipases also provide stereochemical and structural selectivity during the polymerization.[5,6]

Copolymerizations of lactones have been explored as a means to tailor and improve copolymer physical properties, including the thermal transitions, mechanical properties, barrier properties, and even degradation rates.[7,8] While the overall copolymer composition plays an important role, the sequence distribution of comonomers within the polymer backbone controls many properties. Li et al.[7,9] studied the degradation and controlled drug release of poly(lactic-*co*-glycolic acid) microspheres and found that monomer sequence dramatically affects properties. "Random" copolymers exhibited a much stronger burst release and accelerated degradation compared to alternating copolymers, because the homodyads degraded faster than heterodyads. However, in many situations, the copolymerization behavior is not intuitively predictable. For example, in bulk homopolymerizations with the catalyst $Al(O^iPr)_3$, ε-caprolactone (ε-CL) has an apparent rate constant three orders of magnitude larger than L-lactide (LA).[10] However, during copolymerization under the same conditions, LA will react to completion before ε-CL is consumed. The reactivity ratios are $r_{\text{L-LA}} = 17.9$ and $r_{\varepsilon\text{-CL}} = 0.58$.

Lipase-catalyzed copolymerizations of various lactones have been reported, including ε-CL, δ-valerolactone (δ-VL), ω-pentadecalactone, trimethylene carbonate, LA, and glycolide.[11−15] Wang et al.[13] also showed that the reactivity ratios for ε-CL and α-methyl-ε-caprolactone (MCL) differed significantly for metal and enzyme catalysts; the sterically hindered MCL had a dramatically lower reactivity via lipase catalyst. In most of the cases where reactivity ratios were reported, the terminal model was applied with no determination of its applicability. However, when using compositional data, the copolymerization can appear to follow the terminal model when the actual mechanism varies dramatically.[16,17]

Received: December 21, 2012
Accepted: April 4, 2013
Published: April 17, 2013

   dx.doi.org/10.1021/mz300659h | *ACS Macro Lett.* 2013, 2, 375−379

Different techniques are required to accurately characterize the copolymerization mechanism. To fully predict the molecular structure and properties of copolymers, one must have an understanding of the copolymerization mechanism. In certain cases of free radical copolymerization, different copolymerization models have been proposed, such as the penultimate model (for styrene-acrylonitrile, for example),[18] complex participation model (for 1,1-diphenylethylene-methyl acrylate, for example),[19] or the copolymerization with simultaneous depropagation (for α-methylstyrene-methyl methacrylate, for example).[20] The penultimate model is commonly used to account for steric effects and transition state stabilization during propagation.[21]

In our previous work, we demonstrated that terminal model reactivity ratios accurately reflect the composition of enzyme-catalyzed poly(ε-CL-*co*-δ-VL) (PCV) copolymers.[22] In addition, the Meyer-Lowry model of composition drift accurately modeled the monomer consumption during polymerization.[15] Both analytical techniques assumed that the enzyme-catalyzed copolymerizations followed terminal model kinetics. Although the compositional model predictions fit the experimental data very well, deviations in the copolymer microstructure (which have been observed previously for free radical systems[16,17]) could dramatically affect the copolymer properties. In the present work, ε-CL and δ-VL were copolymerized in toluene via immobilized *Candida antarctica* Lipase B (CALB; N435 beads, obtained from Novozymes). (Certain commercial equipment, instruments, or materials are identified in this paper in order to specify the experimental procedure adequately. Such identification is not intended to imply recommendation or endorsement by the National Institute of Standards and Technology, nor is it intended to imply that the materials or equipment identified are necessarily the best available for the purpose.) Scheme 1 illustrates the monomer and copolymer structures. Using ^{13}C NMR spectroscopy, the triad sequence distributions were calculated and compared to theoretical distributions for the terminal and penultimate models.

Scheme 1. Lipase-Catalyzed Copolymerization of ε-CL and δ-VL

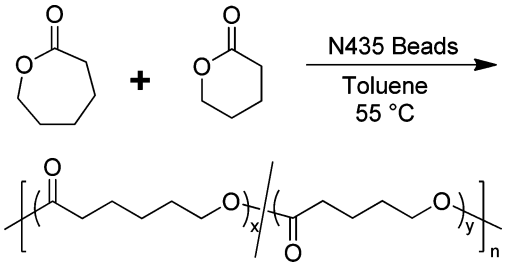

Reactivity ratios were determined from low conversion compositional data from ^{1}H NMR spectra. Figure 1 shows the copolymer composition as a function of comonomer feed composition. The terminal model copolymer composition equation:

$$F_C = \frac{r_C f_C^2 + f_C f_V}{r_C f_C^2 + 2 f_C f_V + r_V f_V^2}$$

relates the copolymer mole fraction of ε-CL, f_C, to the monomer feed fraction of ε-CL, f_C, where r_C and r_V are the reactivity ratios of ε-CL and δ-VL, respectively. The terminal model reactivity ratios were estimated as r_C = 0.56 and r_V = 0.39. The calculated reactivity ratios for the penultimate model were estimated as r_{CC} = 0.46, r_{CV} = 0.46, r_{VC} = 0.26, and r_{VV} = 0.54 using the penultimate model copolymer composition relationship[23]

$$F_C = \frac{r_{VC} f_C^2 \left(\frac{r_{CC} f_C + f_V}{r_{VC} f_C + f_V}\right) + f_C f_V}{r_{VC} f_C^2 \left(\frac{r_{CC} f_C + f_V}{r_{VC} f_C + f_V}\right) + 2 f_C f_V + r_{CV} f_V^2 \left(\frac{r_{VV} f_V + f_C}{r_{CV} f_V + f_C}\right)}$$

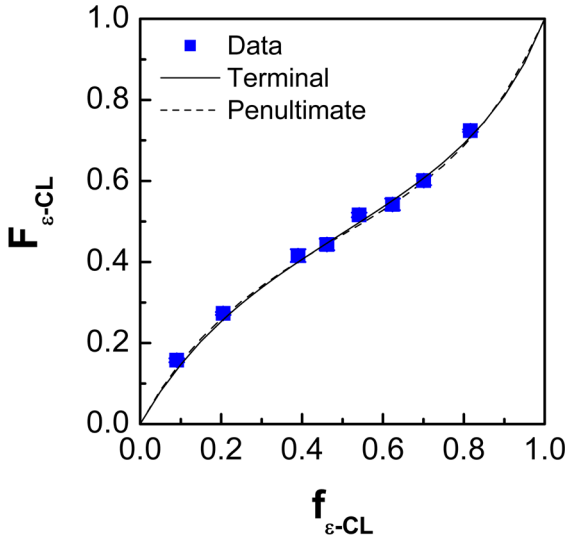

Figure 1. Copolymer composition ($F_{\varepsilon\text{-CL}}$) of PCV copolymers as a function of monomer feed fraction ($f_{\varepsilon\text{-CL}}$), determined by ^{1}H NMR spectroscopy in $CDCl_3$: (■) Experimental data, (−) terminal model predictions, and (--) penultimate model predictions. Error bars (covered by symbols) for the experimental data represent one standard deviation based on the measurement of at least three samples.

The theoretical copolymer composition curves for both terminal and penultimate models are shown in Figure 1. It is apparent that both models fit the compositional data very well, even at high and low monomer ratios. For this model system, composition does not effectively discriminate between kinetic models.

The ^{13}C NMR spectra in $CDCl_3$ for homopolymers and copolymers are shown in Figure 2, expanded around 64 ppm, for the region corresponding to the methylene adjacent the ester oxygen. The copolymers exhibit four distinct peaks corresponding to the different dyad sequences. These dyads have been previously identified[24] and are labeled within Figure 2. Intuitively, the fraction of homodyads is highest in the copolymers rich in either ε-CL or δ-VL. The heterodyads become prevalent in the intermediate compositions. The dyad splitting was also well resolved in all other carbon peaks, but the methylene signal around 64 ppm was chosen for analysis because the separation between peaks was largest. The complete ^{13}C NMR spectrum and additional expansions are included in the electronic Supporting Information.

The kinetic models of copolymerization allow prediction of dyad and triad fractions based solely on the reactivity ratios and feed composition. Because the shortest defined sequence in the penultimate model is a triad, the terminal model is expanded to triad sequences as well for an equivalent comparison. The ε-

dx.doi.org/10.1021/mz300659h | ACS Macro Lett. 2013, 2, 375−379

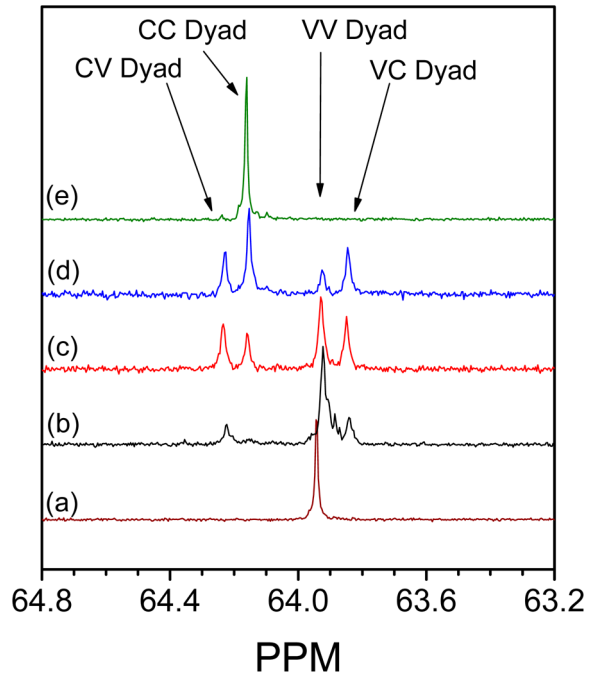

Figure 2. Expansion of the ^{13}C NMR spectra of PCV copolymers with initial feed composition $f_{\varepsilon\text{-CL},0}$ of (a) 0.0, (b) 0.1, (c) 0.3, (d) 0.6, and (e) 1.0.

CL-centered triad probabilities for the terminal model are given by[23]

$$P_{CCC} = \frac{r_C^2 f_C^2}{r_C^2 f_C^2 + 2 r_C f_C f_V + f_V^2}$$

$$P_{CCV} = P_{VCC} = \frac{r_C f_C f_V}{r_C^2 f_C^2 + 2 r_C f_C f_V + f_V^2}$$

$$P_{VCV} = \frac{f_V^2}{r_C^2 f_C^2 + 2 r_C f_C f_V + f_V^2}$$

The probabilities are defined such that the sum of P_{CCC}, P_{CCV}, P_{VCC}, and P_{VCV} equals 1. Expressions for the δ-VL-centered triads have a similar structure. The ε-CL-centered triad probabilities for the penultimate model are given by[23]

$$P_{CCC} = \frac{r_{VC} r_{CC} f_C^2}{r_{VC} r_{CC} f_C^2 + 2 r_{VC} f_C f_V + f_V^2}$$

$$P_{CCV} = P_{VCC} = \frac{r_{VC} f_C f_V}{r_{VC} r_{CC} f_C^2 + 2 r_{VC} f_C f_V + f_V^2}$$

$$P_{VCV} = \frac{f_V^2}{r_{VC} r_{CC} f_C^2 + 2 r_{VC} f_C f_V + f_V^2}$$

Experimental dyad fractions can be obtained from the integrated areas of the NMR spectra. Dyad probabilities are defined as the fraction of ε-CL-terminated propagating chains which form either CC or CV dyads (P_{CC} and P_{CV}, respectively). P_{VV} and P_{VC} are defined likewise. The dyad fractions are related to the peak areas as

$$P_{CC} = \frac{A_{CC}}{A_{CC} + A_{CV}}$$

$$P_{CV} = \frac{A_{CV}}{A_{CC} + A_{CV}}$$

Triad fractions are calculated as the joint probabilities of the corresponding dyad probabilities. The experimental ε-CL-centered triad probabilities are defined as

$$P_{CCC} = P_{CC} \times P_{CC}$$

$$P_{CCV} = P_{CC} \times P_{CV}$$

$$P_{VCV} = P_{VC} \times P_{CV}$$

Figure 3 shows the ε-CL-centered triad fractions determined by ^{13}C NMR analysis as well as the theoretical predictions for

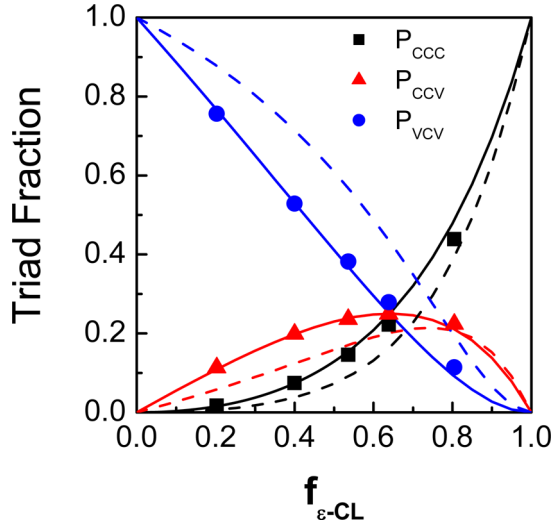

Figure 3. Caprolactone-centered triad fractions for enzyme-catalyzed copolymers: (■) CCC triad, (▲) CCV triad, and (●) VCV triad. The symbols represent experimental data and the lines represent (−) terminal and (--) penultimate model predictions. Error bars (covered by the symbols) for the experimental data represent one standard deviation based on the measurement of at least three samples.

the terminal and penultimate models. The overall number of ε-CL-centered triads is not constant and increases with increased ε-CL content of the copolymers. These triad fractions simply represent the percentage of the total caprolactone-centered triads. The experimental triad fractions clearly agree very well with the terminal model predictions.

Like the conventional linearization techniques to determine reactivity ratios, the analysis of triad probabilities assumes a constant feed ratio. Therefore, the analysis must be performed at low conversions to determine the instantaneous sequence distribution. At higher conversions the feed composition may drift and the sequence distributions will tend toward a composite average. In the results discussed above, all polymerizations were stopped at low conversions and the polymers were precipitated, isolated, and analyzed. However, precipitation often leads to fractionation, and enzymatic polymerizations are known to generate large fractions of cyclic oligomers at low conversion.[2] To investigate the impact of precipitation, we performed the polymerization in toluene-d_8 and collected aliquots at low conversion to analyze directly via ^{13}C NMR spectroscopy. Figure 4 shows the NMR spectra of

dx.doi.org/10.1021/mz300659h | ACS Macro Lett. 2013, 2, 375−379

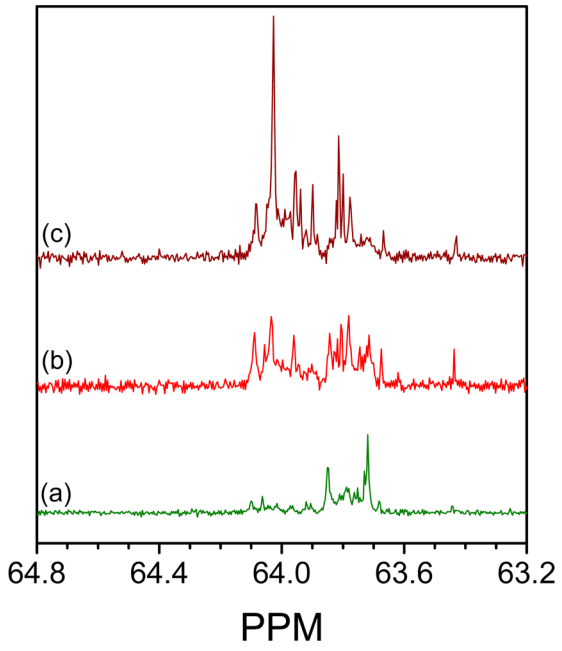

Figure 4. ^{13}C NMR spectra of PCV copolymerization reaction mixture in toluene-d_8 with nominal $f_{\varepsilon\text{-CL},0}$ of (a) 0.1, (b) 0.4, and (c) 0.7.

the reaction aliquots for homo- and copolymers, also expanded to show the region around 64 ppm. Numerous overlapping peaks are observed, presumably resulting from a complex mixture of low molar mass cyclic and linear oligomers. However, relative areas of the ε-CL region (63.85 to 64.20 ppm) and the δ-VL region (63.60 to 63.85 ppm) correspond to the relative ratios of ε-CL and δ-VL in the precipitated copolymers. This suggests that, although the precipitation process eliminates many of the cyclic oligomers, the overall population is still well represented.

In summary, the microstructure of CALB-catalyzed PCV copolymers was found to conform to terminal model kinetics. ^{13}C NMR spectroscopy enabled the rapid determination of dyad fractions in the copolymers, serving as a useful tool for characterizing copolymer structures. Although compositional analysis was not able to discriminate between terminal and penultimate copolymerization models, the sequence analysis elucidated strong differences between the two models. Future work should focus on extending this technique to other monomer pairs, especially the sterically crowded monomers, such as LA or MCL, which may not necessarily follow terminal model kinetics. This technique will enable more effective predictive analysis of the properties of enzyme-catalyzed aliphatic polyesters.

EXPERIMENTAL SECTION

Toluene, toluene-d_8, ε-CL, and δ-VL were obtained from Sigma-Aldrich and distilled over CaH_2 prior to use. δ-VL was stored at 0 °C to prevent autopolymerization. $CDCl_3$ was obtained from Cambridge Isotope Laboratories, Inc. and used as received. N435 catalyst beads were obtained from Novozymes (Bagsvaerd, Denmark) and stored in a vacuum desiccator prior to use. To minimize deviations caused by variations in N435 particle size, a 400 μm sieve was used to select a particle size distribution of 400 μm ± 50 μm. All copolymerizations were performed according to previously reported procedures.[20]

NMR spectra were obtained at 298 K on a Bruker AVANCE 600 MHz spectrometer (Bruker-Biospin, Billerica, MA) equipped with a 5 mm z-gradient broadband probe. Already available standard Bruker experimental setup was optimized to acquire directly detected ^{13}C spectra with proton decoupling. 1D-^{13}C data sets were recorded at 150.918 MHz using 512 scans of 65536 data points with a prescan delay of 2 s and a spectral width of 240 ppm. Initial experiments estimated the T_1 relaxation time for the ^{13}C spectra as less than 0.5 s. All spectra were referenced to the toluene-d_8 resonance at 137.89 ppm.

ASSOCIATED CONTENT

Supporting Information

Complete ^{13}C NMR spectra and expanded regions. This material is available free of charge via the Internet at http://pubs.acs.org.

AUTHOR INFORMATION

Corresponding Author

*E-mail: beers@nist.gov.

Notes

The authors declare no competing financial interest.

ACKNOWLEDGMENTS

The authors would like to acknowledge the support of the National Research Council Postdoctoral Fellowship Program.

REFERENCES

(1) Kobayashi, S. *Macromol. Rapid Commun.* **2009**, *30*, 237−266.
(2) Johnson, P. M.; Kundu, S.; Beers, K. L. *Biomacromolecules* **2011**, *12*, 3337−3343.
(3) Bhangale, A. S.; Beers, K. L.; Gross, R. A. *Macromolecules* **2012**, *45*, 7000−7008.
(4) Yang, Y.; Yu, Y.; Zhang, Y.; Liu, C.; Shi, W.; Li, Q. *Process Biochem.* **2011**, *46*, 1900−1908.
(5) Van Buijtenen, J.; van As, B. A. C.; Verbruggen, M.; Roumen, L.; Vekemans, J. A. J. M.; Pieterse, K.; Hilbers, P. A. J.; Hulshof, L. A.; Palmans, A. R. A.; Meijer, E. W. *J. Am. Chem. Soc.* **2007**, *129*, 7393−7398.
(6) Peeters, J.; Palmans, A. R. A.; Veld, M.; Scheijen, F.; Heise, A.; Meijer, E. W. *Biomacromolecules* **2004**, *5*, 1862−1868.
(7) Li, J.; Rothstein, S. N.; Little, S. R.; Edenborn, H. M.; Meyer, T. Y. *J. Am. Chem. Soc.* **2012**, *134*, 16352−16359.
(8) Cao, A.; Okamura, T.; Ishiguro, C.; Nakayama, K.; Inoue, Y.; Masuda, T. *Polymer* **2002**, *43*, 671−679.
(9) Li, J.; Stayshich, R. M.; Meyer, T. Y. *J. Am. Chem. Soc.* **2011**, *133*, 6910−6913.
(10) Vion, J. M.; Jerome, R.; Teyssie, P.; Aubin, M.; Prudhomme, R. E. *Macromolecules* **1986**, *19*, 1828−1838.
(11) Jiang, Z.; Azim, H.; Gross, R. A.; Focarete, M. L.; Scandola, M. *Biomacromolecules* **2007**, *8*, 2262−2269.
(12) Kumar, A.; Garg, K.; Gross, R. A. *Macromolecules* **2001**, *34*, 3527−3533.
(13) Wang, C.; Xiao, Y.; Heise, A.; Lang, M. *J. Polym. Sci., Part A: Polym. Chem.* **2011**, *49*, 5293−5300.
(14) Lassalle, V.; Galland, G.; Ferreira, M. *Bioproc. Biosys. Eng.* **2008**, *31*, 499−508.
(15) Hunley, M. T.; Beers, K. L. *Macromolecules* **2013**, *46*, 1393−1399.
(16) Fukuda, T.; Ma, Y. D.; Inagaki, H.; Kubo, K. *Macromolecules* **1991**, *24*, 370−375.
(17) Ma, Y.-D.; Sung, K.-S.; Tsujii, Y.; Fukuda, T. *Macromolecules* **2001**, *34*, 4749−4756.
(18) Hill, D. J. T.; O'Donnell, J. H.; O'Sullivan, P. W. *Macromolecules* **1982**, *15*, 960−966.
(19) Cais, R. E.; Farmer, R. G.; Hill, D. J. T.; O'Donnell, J. H. *Macromolecules* **1979**, *12*, 835−839.
(20) Palmer, D. E.; McManus, N. T.; Penlidis, A. *J. Polym. Sci., Part A: Polym. Chem.* **2000**, *38*, 1981−1990.
(21) Heuts, J. P. A.; Gilbert, R. G.; Maxwell, I. A. *Macromolecules* **1997**, *30*, 726−736.

(22) Hunley, M. T.; Bhangale, A. S.; Kundu, S.; Johnson, P. M.; Waters, M. S.; Gross, R. A.; Beers, K. L. *Polym. Chem.* **2012**, *3*, 314−318.
(23) Burke, A. L.; Duever, T. A.; Penlidis, A. *Macromolecules* **1994**, *27*, 386−399.
(24) Shin, E. J.; Brown, H. A.; Gonzalez, S.; Jeong, W.; Hedrick, J. L.; Waymouth, R. M. *Angew. Chem., Int. Ed.* **2011**, *50*, 6388−6391.